Supplementary materials

Table S1 – List of samples, collection date, temperature and mineralogical associations as resulting by XRDP analyses corroborated by FTIR and EDS-BSEM study. The sampling includes water spring sampled at Stufe di Nerone. In the temperature column: tc, thermo couple (see chapter 2.2 Sampling, sample preparation and analytical techniques), infr, infrared gun. In the mineralogy column: ?, for minerals to be validated; minerals in red are approximate attribution based on XRDP patterns. The orange cells evidence water samples. Representative XRDP spectra are in Fig. S1. Further details in this supplement.

Sample name	Sampled area	Location*	Details on sites and sample	Temperature (°C) tc, infr	Sampling date	Mineralogy	pH	Note
Ss1	Pisciarelli	L1	-	-	09-Jan-13	Sulfur	nd	Piochi et al 2015
S_{tot}2	Pisciarelli	L1	-	-	09-Jan-13	Pickeringite, Alunite, Alunogen, Alum-(K), Sulfur, Amarillite, Mereiterite	nd	Piochi et al 2015
S3	Pisciarelli	L1	-	-	09-Jan-13	Alunite, Alum-(K)	nd	Piochi et al 2015
S_{tot}4	Pisciarelli	L1	-	-	09-Jan-13	Alunogen, Alunite, Sulfur, Kaolinite	nd	Piochi et al 2015
S5	Pisciarelli	L2	-	-	09-Jan-13	Quartz, Amorphous	nd	Piochi et al 2015
S7	Pisciarelli	L2	-	-	09-Jan-13	Alunite, Alunogen, Illite/Montmorillonite	nd	Piochi et al 2015
S10	Pisciarelli	L2	-	-	21-Mar-13	Alunite, Illite/Montmorillonite	nd	Piochi et al 2015
Sf12	Pisciarelli	L3 - mud pool	mud	-	21-Mar-13	Alunite, Sulfur, K-Feldspar, Amorphous, Illite	nd	Piochi et al 2015
Sf14	Pisciarelli	L3 - mud pool	mud	-	10-Oct-13	Alunite Sulfur, K-Feldspar, Amorphous, Illite	nd	Piochi et al 2015
S_{tot}16	Pisciarelli	L4	-	-	21-Mar-13	Quartz, Amorphous, Illite/Montmorillonite, Kaolinite	nd	Piochi et al 2015
ASA 12-3	Solfatara	ASA	NE-slope, uppermost part	-	11-Dec-13	Alunite, Alunogen	nd	Piochi et al 2015
AP 12-3	Pisciarelli	L1	-	-	11-Dec-13	Alunite, Alunogen, Alum-(K)	nd	Piochi et al 2015

MP^	Pisciarelli	L3 - mud pool	mud	-	11-Dec-13	Alunite, Sulfur K-Feldspar, Amorphous, Illite	nd	Piochi et al 2015
MS	Solfatara	pool	mud	-	11-Dec-13	Alunite, Sulfur K-Feldspar, Amorphous, Illite	nd	Piochi et al 2015
Red_1_1/15	Pisciarelli	L50	reddish deposits	-	29-Jan-15	Alunite, Hematite	nd	Piochi et al 2015
Sg12	Pisciarelli	L3 - mud pool	separated from the mud	-	17-Apr-13	Gypsum	nd	Piochi et al 2015
Lava	Solfatara	L5	NW area from Stuff, dome	-	24-Jun-14	Alunite, Analcime, Quartz	nd	Piochi et al 2015
Tephra	Solfatara	L5	NW area from Stuff	-	24-Jun-14	Analcime, Quartz, Gypsum, Illite	nd	Piochi et al 2015
S8	Pisciarelli	L2	-	-	09-Jan-13	Alunite	nd	Piochi et al 2015
S9	Pisciarelli	L2	-	-	11-Mar-13	Sulfur	nd	Piochi et al 2015
Ss15	Pisciarelli	L4	-	-	21-Mar-13	Sulfur	nd	Piochi et al 2015
Sp13	Pisciarelli	L3 - mud pool	separated from the mud	-	17-Apr-13	Pyrite	nd	Piochi et al 2015
ASA 24-9	Solfatara	ASA	NE-slope, uppermost part	-	24-Sep-14	Alunite	nd	Piochi et al 2015
AP 24-9_2b	Pisciarelli	L1	-	-	24-Sep-14	Alunite	nd	Piochi et al 2015
AP 24-9_2a	Pisciarelli	L1	-	-	24-Sep-14	Alunite	nd	Piochi et al 2015
AP 24-9	Pisciarelli	L1	-	-	24-Sep-14	Alunite	nd	Piochi et al 2015
ASA 12-3	Solfatara	ASA	NE-slope, uppermost height	-	11-Dec-13	Alunite	nd	Piochi et al 2015
AP 12-3	Pisciarelli	L1	-	-	09-Jan-13	Alunite	nd	Piochi et al 2015
Sample 2 alunite	Pisciarelli	L1	-	-	09-Jan-13	Alunite	nd	Piochi et al 2015
SSA 24-9 S	Solfatara	ASA	NE-slope, uppermost height	-	24-Sep-14	Sulfur	nd	Piochi et al 2015
SS 24-9 bg S	Solfatara	Bocca Grande	-	-	24-Sep-14	Sulfur	nd	Piochi et al 2015
SS 24-9b S	Solfatara	ASA	NE-slope, lowermost height	-	24-Sep-14	Sulfur	nd	Piochi et al 2015

SS 24-9i S	Solfatara	ASA	NE-slope, intermediate height	-	24-Sep-14	Sulfur		nd		Piochi et al 2015
SP 24-9 S	Pisciarelli	L1	-	-	24-Sep-14	Sulfur		nd		Piochi et al 2015
SP 12-3	Pisciarelli	L1 vent	-	-	11-Dec-13	Sulfur		nd		Piochi et al 2015
SS 12-3 b	Solfatara	ASA	NE-slope, lowermost height	-	11-Dec-13	Sulfur		nd		Piochi et al 2015
SS 12-3 i	Solfatara	ASA	NE-slope, intermediate height	-	11-Dec-13	Sulfur		nd		Piochi et al 2015
SSA 12-3	Solfatara	ASA	NE-slope, uppermost height	-	11-Dec-13	Sulfur		nd		Piochi et al 2015
SS 12-13 BG	Solfatara	Bocca Grande	-	-	11-Dec-13	Sulfur		nd		Piochi et al 2015
Sample 6 Sulfur	Pisciarelli	L1	-	-	09-Jan-13	Sulfur		nd		Piochi et al 2015
Sample 11 Sulfur	Pisciarelli	L4	-	-	09-Jan-13	Sulfur		nd		Piochi et al 2015
Sample 4 Sulfur	Pisciarelli	L1	-	-	09-Jan-13	Sulfur		nd		Piochi et al 2015
Sample 2 Sulfur	Pisciarelli	L1	-	-	09-Jan-13	Sulfur		nd		Piochi et al 2015
MS 24-9 Ag2S - elemental S	Solfatara	Mud pool	separated from mud	-	24-Sep-14	Sulfur in the mud		nd		Piochi et al 2015
MP 24-9 Ag2S - elemental S	Pisciarelli	Mud pool	separated from mud	-	24-Sep-14	Sulfur in the mud		nd		Piochi et al 2015
Geiser Mud - elemental S	Pisciarelli	Opened Geiser	-	-	11-Dec-13	Sulfur in the mud		nd		Piochi et al 2015
Solfatara - elemental S	Solfatara	Mud pool	separated from mud	-	09-Feb-13	Sulfur in the mud		nd		Piochi et al 2015
MP 12-3 - elemental S	Pisciarelli	Mud pool	separated from mud	-	11-Dec-13	Sulfur in the mud		nd		Piochi et al 2015
MS 12-3 - elemental S	Solfatara	Mud pool	separated from mud	-	11-Dec-13	Sulfur in the mud		nd		Piochi et al 2015
Geiser Mud CRS+AVS	Pisciarelli	Opened Geiser	-	-	01-Mar-14	Bulk mud		nd		Piochi et al 2015
Solfatara CRS+AVS	Solfatara	Mud pool	-	-	01-May-13	Bulk mud		nd		Piochi et al 2015

MP 12-3 CRS+AVS	Pisciarelli	L3 - mud pool	mud	-	11-Dec-13	Bulk mud	nd	Piochi et al 2015
MS 12-3 CRS+AVS	Solfatara	Mud pool	-	-	11-Dec-13	Bulk mud	nd	Piochi et al 2015
L1c S/11-15	Pisciarelli	L1 vent	cream-like	90.1	09-Nov-15	-	nd	-
L1a S/11-15	Pisciarelli	L1 wall	minute Sulfur crystals	-	09-Nov-15	-	nd	-
L1d wr/11-15	Pisciarelli	L1 wall	whole-rock	-	09-Nov-15	Alunogen	nd	-
L1d1 al/11-15	Pisciarelli	L1 wall	hot soft white efflorescence (neve calda)	-	09-Nov-15	Alunogen, Meta-alunogen, Amorphous	nd	-
L1d2 white/11-15	Pisciarelli	L1 wall	white	-	09-Nov-15	Ammonium sulfate, Alunogen, Amorphous	nd	-
MP/11-15	Pisciarelli	Mud pool	black mud	-	09-Nov-15	Alunite, Sulfur, K-feldspar, Pyrite, Mica/Clay, Amorphous	nd	-
P PP/11-15	Pisciarelli	Opened Geiser	argilla	52	09-Nov-15	nd	nd	-
P PP1/11-15	Pisciarelli	Opened Geiser	argilla	92°C	09-Nov-15	Sulfur, Amorphous, Pyrite, Clay, Alum-(K)	nd	-
P PPv/11-15	Pisciarelli	L19 Geiser-pool wall	green	34.2	09-Nov-15	Sulfur, Ammonium sulfate (mascagnite type), Alunite, Amorphous	nd	-
P PPb/11-15	Pisciarelli	L19 Geiser-pool wall	beige	50.2	09-Nov-15	Alunite, Amorphous	nd	-
P Pv/11-15	Pisciarelli	L20 new vents	argilla	60.5	09-Nov-15	Sulfur, Ammonium sulfate, Alunite, Montmorillonite	nd	-
P L50 yellow	Pisciarelli	L50 - high NW slope	yellow ashy-to-sandy deposits	-	09-Nov-15	Jarosite, Chabazite?, Alunite, Amorphous	nd	-
P L50 white	Pisciarelli	L50 - high NW slope	white ashy-to-sandy deposits	-	09-Nov-15	Alunite, Clay?, Amorphous	nd	-
P L50 red	Pisciarelli	L50 - high NW slope	reddish ashy-to-sandy deposits	-	09-Nov-15	Fe-oxide, Jarosite, Alunite, Amorphous	nd	-
SP/11-15	Solfatara	Mud pool	mud	76.7	09-Nov-15	-	nd	-

BG wr/11-15	Solfatara	Bocca Grande	yellow and black portion at fumarole	93.1	09-Nov-15	Pyrite, hight Amorphous content	nd	-
BG pg/11-15	Solfatara	Bocca Grande	yellow portion at fumarole above	-	09-Nov-15	Sulfur	nd	-
SStg/11-15	Solfatara	SSt- Stuff	light yellow S	63.5-93	09-Nov-15	Sulfur	nd	-
SStb/11-15	Solfatara	SSt- Stuff	whitish	63.5-93	09-Nov-15	Alunite, Alunogen, As-Fe bearing phases, Amorphous	nd	-
SStgf/11-15	Solfatara	SSt- Stuff	yellow S crystals	63.5-93	09-Nov-15	Sulfur	nd	-
SStgc/11-15	Solfatara	SSt- Stuff	columnar S	-	09-Nov-15	Sulfur	nd	-
L1v PSc/6-16	Pisciarelli	L1vent	crystalline	>87	14-Jun-16	Sulfur	nd	-
L1v PGw/6-16	Pisciarelli	L1 vent	gray lenses	>87	14-Jun-16	Amorphous, bad spectrum	nd	-
L1v PSg/6-16	Pisciarelli	L1 vent	S liquid?	>87	14-Jun-16	very strange pattern	nd	-
L1v Pwc/6-16	Pisciarelli	L1 vent	cream-like	>87	14-Jun-16	Sulfur, Sb-sulfide, Fe-oxide	nd	-
L1 Pv/6-16	Pisciarelli	L1 wall	vitreous	56.9	14-Jun-16	Clay, Alunite, Quartz, Amorphous	nd	-
L1 PvSc/6-16	Pisciarelli	L1 wall	vitreous	56.9	14-Jun-16	Sulfur	nd	-
L1 Pwh/6-16	Pisciarelli	L1 wall	-	56.9	14-Jun-16	-	nd	-
L1 Psalt/6-16	Pisciarelli	L1 wall	saline crust	67	14-Jun-16	Alum-(K), Alunogen	nd	-
L1Pblack/6-16	Pisciarelli	L1 wall	blackish, at a fracture on wall	67	14-Jun-16	Sulfur plus beta sulfur (shifted pattern), Amorphous	nd	-
MP/6-16	Pisciarelli	L3 - mud pool	mud	>70	14-Jun-16	Alunite, Sulfur, K-feldspar, Illite, Amorphous	nd	-
Geiser mud	Pisciarelli	Opened Geiser	argilla	>90	14-Jun-16	Halotrichite?, Sulfur, Alunite, Illite/montmorillonite, Amorphous	nd	-
GnvW bl/6-16	Pisciarelli	L19 Geiser-pool wall	black argilla	74.7	14-Jun-16	Alunite, Sb-sulfur, Amorphous	nd	-

GnvW be/6-16	Pisciarelli	L19 Geiser-pool wall	plastered beige argilla	74.7	14-Jun-16	Mascagnite, Alunite, Arseniate or Phosphate, Amorphous	nd	-
P L20 v1/6-16	Pisciarelli	L20 new vent1	gray argilla	90	14-Jun-16	Mascagnite, Alunite, Illite/montmorillonite, Amorphous	nd	-
P L20 v2 S/6-16	Pisciarelli	L20 new vent2	Sulfur	44	14-Jun-16	Sulfur (Beta sulfur)	nd	-
P L50 white/6-16	Pisciarelli	L50 - high NW slope	white ashy-to-sandy deposits	-	14-Jun-16	Alunite, Alum-(Na), Minamiite?, Amorphous	nd	-
P L50 yellow/6-16	Pisciarelli	L50 - high NW slope	yellow ashy-to-sandy deposits	-	14-Jun-16	Alunite, Coquimbite?, Amorphous	nd	-
P L50 black/6-16	Pisciarelli	L50 - high NW slope	black ashy-to-sandy deposits	-	14-Jun-16	Jarosite, Alunite, Gypsum, Amorphous	nd	-
P L20 Nnv/6-16	Pisciarelli	L20 - wall N of new vents	-	94	14-Jun-16	-	nd	-
PS/6-16	Solfatara	Mud pool	mud	52.9	14-Jun-16	Sulfur, Alunite, Anorthoclase, Amorphous	nd	-
BG S/6-16	Solfatara	Bocca Grande	S cream-like	93.2	14-Jun-16	Sulfur	nd	-
up BG S/6-16	Solfatara	BG-nearby area	crystalline sulfur	93.2	14-Jun-16	Sulfur	nd	-
buco a/6-16	Solfatara	BUCO	orange portion into the hole	-	14-Jun-16	Sulfur (new type-cif), Ammonium Hydrogen Arsenate	nd	-
SMO ASA/6-16	Solfatara	SMO	white, Monte Olibano	87	14-Jun-16	Sulfur, Alunite, Amorphous	nd	-
SMO S/6-16	Solfatara	SMO	fine yellow, Monte Olibano	87	14-Jun-16	Sulfur	nd	-
ASA m/16-6	Solfatara	ASA	white on the NE-slope, intermediate height	-	14-Jun-16	Sulfur, Pyrite, Amorphous	nd	-
ASA h/16-6	Solfatara	ASA	white on the NE-slope,	-	14-Jun-16	Sulfur, Alunite, Cu-mineral?, Amorphous	nd	-

			uppermost height					
SS/16-6	Solfatara	SSt - NE-low	sulfur	-	14-Jun-16	Sulfur	nd	-
SSt Sf/16-6	Solfatara	SSt- Stuff	Sulfur in fracture	92	14-Jun-16	Sulfur	nd	-
SSt Sp/16-6	Solfatara	SSt- Stuff	Sulfur as fluff	92	14-Jun-16	Sulfur	nd	-
SSt w/16-6	Solfatara	SSt- Stuff	white	45	14-Jun-16	Alunogen, Clay (montmorillonite?), Gypsum	nd	-
SSt sub/16-6	Solfatara	SSt- Stuff	substratum of sulfur	92	14-Jun-16	Periclase (MgO), Alunite, Quartz, Amorphous	nd	-
SSt win/16-6	Solfatara	SSt- Stuff	efflorescence within Stuff	-	14-Jun-16	Rostite Al $(SO_4)(OH)\cdot 5H_2O$, Sb-sulfide, Quartz, Amorphous	nd	-
Ps 7-16*	Pisciarelli	L3 - mud pool	mud	-	28-Jul-16	Sulfates plus Sulfur, clay (illite), Amorphous	nd	-
PL 20V1 7-16*	Pisciarelli	L20	gray argilla	-	28-Jul-16	SO_4 (mascagnite), few illite	nd	-
L3-2	Pisciarelli	L3 - vent neaby mud pool	efflorescence	-	20-Sep-16	Alunite, Sulfur K-Feldspar, Amorphous, Pyrite, Coquimbite	nd	-
L1-7	Pisciarelli	L1 vent	efflorescence	-	20-Sep-16	Alunite, Sulfur, Pyrite, Quartz, Amorphous	nd	-
L1-6	Pisciarelli	L1 vent	efflorescence	>95	20-Sep-16	Sulfur, Quartz, Amorphous	nd	-
S BG	Solfatara	Bocca Grande	Yellowish sulfur impregnating widely covers the greenish efflorescence	-	20-Sep-16	Sulfur, Quartz, Amorphous	nd	-
L3-2	Pisciarelli	L3 - vent neaby mud pool	Gray portion	84.4	20-Sep-16	Alunite, Sulfur, K-Feldspar, Amorphous	nd	-
Smudbag	Solfatara	Mud pool	Beidge mud	-	20-Sep-16	Alunite, Sulfur, K-Feldspar, Amorphous	nd	-

Smudtube	Solfatara	Mud pool	Beidge mud	50.4	20-Sep-16	Alunite, Sulfur, K-Feldspar, Amorphous	nd	-
Smud box	Solfatara	Mud pool	Beidge mud	35-43	20-Sep-16	Alunite, Sulfur, K-Feldspar, Amorphous	nd	-
MP 09/16	Pisciarelli	L3 - Mud pool	Beidge mud	-	20-Sep-16	Alunite, Sulfur, K-Feldspar, Pyrite, Amorphous	nd	-
L1-3 greenish	Pisciarelli	L1 vent	greenish efflorescence	29.8	20-Sep-16	-	nd	-
MP/2-17	Pisciarelli	L3 - Mud pool	gray mud	-	03-Feb-17	Alunite, Sulfur, K-Feldspar, Pyrite, Amorphous	nd	-
L1-SP2-17	Pisciarelli	L1 vent	sulfur cream, very hot	-	03-Feb-17	Sulfur	nd	-
L1-AP2-17	Pisciarelli	L1 vent	efflorescence	-	03-Feb-17	Alunite, Alunogen	nd	-
L1-SP2-17 low	Pisciarelli	L1 vent	sulfur acicular	-	03-Feb-17	Sulfur	nd	-
L1-SP3-17	Pisciarelli	L1 vent in fracture	Sulfur acicular efflorescence	-	03-Feb-17	Sulfur	nd	-
MP/04-17	Pisciarelli	L3 - Mud pool	gray mud	-	06-Apr-17	Alunite, Sulfur, K-Feldspar, Pyrite, Amorphous	nd	-
MS/04-17	Solfatara	Mud pool	Beidge mud	-	06-Apr-17	Alunite, Sulfur, K-Feldspar, Amorphous	nd	-
MPS 517 new	Solfatara	Mud pool	grey mud	-	31-May-17	Kaolinite, Alunite, Sulfur, K-Feldspar, Amorphous (Mascagnite, Sulfur, mica in the surnatant)	nd	-
Buco a/517	Solfatara	BUCO	orange portion in the hole	-	31-May-17	Sulfur	nd	-
L1-S517	Pisciarelli	L1 vent near green portion	efflorecence	-	31-May-17	Sulfur	nd	-
L1-S517 high	Pisciarelli	L1 vent	sulfur cream, very hot	-	31-May-17	Sulfur	nd	-

BG S/517	Solfatara	Bocca Grande	sulfur	-	31-May-17	Sulfur	nd	-
MS/517	Solfatara	Mud pool	Beije mud	-	31-May-17	Sulfur, Alunite , Hydrobiotite/Illite?, Amorphous	nd	-
MP/2906-17	Pisciarelli	L3 - Mud pool	gray mud	-	29-Jun-17	Alunite, Sulfur, K-Feldspar, Pyrite, Amorphous, Illite, Alum-(Na)	nd	-
MS/2906-17	Solfatara	Mud pool	Beije mud	-	29-Jun-17	Sulfur, Alunite, Amorphous, Illite? bad XRD pattern	nd	-
MS new/2906-17	Solfatara	Mud pool	Beije mud	-	29-Jun-17	Sulfur, Alunite, Alum-(Na), Kaolinite, Amorphous	nd	-
L60 24/7/17	Pisciarelli	L60	Sulfur at the level of the bubbling aquifer in a narrow hole	83.6	24-Jul-17	Sulfur	nd	-
L3 24/7/17	Pisciarelli	L3 - mud pool	mud, central mud pool	76.1	24-Jul-17	Sulfur, Gypsum, K-mascagnite	nd	-
L1 main 24/7/17	Pisciarelli	L1 vent	Blackish with sulfur	>92	24-Jul-17	Sulfur, Pyrite, Amorphous	nd	-
L20 new vent 24/7/17	Pisciarelli	L20 high area	high area south of pool, blackish with S modified from gray	>86	24-Jul-17	Sulfur, Alunite, Gypsum, Amorphous	nd	-
L20 bombola	Pisciarelli	L20 high area	high area south of pool, whitish	47	24-Jul-17	Mascagnite, Illite, Amorphous	nd	-
PEXT	Pisciarelli	PEXT	yellowish crystalline Sulfur	95	24-Jul-17	Sulfur (bad pattern)	nd	-
MS 24/7/17	Solfatara	mud pool	mud, mostly dried portion	48.1	24-Jul-17	Sulfur, Alunite, Sanidine, Pyrite, low Amorphous	nd	-
BG 24/7/17	Solfatara	Bocca Grande	Blackish with sulfur	92	24-Jul-17	Sulfur, As species?	nd	-

MS new	Solfatara	new pool	liquid and oily mud	-	24-Jul-17	Minamiite, Alunite, K-Feldspar, Amorphous, Kaolinite, bad pattern	nd	-
Buco 24/7/17	Solfatara	BUCO	orange portion in the hole	-	24-Jul-17	Sulfur, Amorphous. bad pattern	nd	-
MP viadotto 9/17	Pisciarelli	viadotto	dried at the foot valley, mud at the inflow area	49.7	01-Sep-17	Sulfur, Alunite, Illite, Amorphous (low abundance)	nd	-
L3 9/17	Pisciarelli	L3 - mud pool	mud from the bubbling point of the pool, drying	63.9-75.6	01-Sep-17	-	nd	-
L1 wall2 zucch 9/17	Pisciarelli	L1 wall	upper part, soft efflorescence	45.1	01-Sep-17	Alunogen (pattern slightly shifted)	nd	-
L1 wall1 9/17	Pisciarelli	L1 wall	between vent and wall 2, white massive with halos	43.7	01-Sep-17	Sulfur, Alunogen	nd	-
L1 vent 9/17	Pisciarelli	L1 vent	blackish-brownish, low Sulfur	>85	01-Sep-17	Sulfur, Alunite, Pyrite, Amorphous	nd	-
L1 wall 1S 9/17_sep bianco	Pisciarelli	L1 wall	sulfur at the wall base	77.5	01-Sep-17	Sulfur, Alunogen	nd	-
L1 wall 1S 9/17_sep S	Pisciarelli	L1 wall	sulfur at the wall base	77.5	01-Sep-17	Sulfur, Alunogen	nd	-
L20 bombola 9/17	Pisciarelli	L20 high area	high area south of pool, low abundance of whitish material	52.9	01-Sep-17	Mascagnite, Alum-(K), Illite	nd	-
MS1 9/17	Solfatara	mud pool	south portion, fine and mellow mud	49.9-48.6	01-Sep-17	Sulfur, Alunite	nd	-
MP L3boccetta 1.9.17	Pisciarelli	L3 - mud pool	mud from the bubbling point centre of the pool	49.9-48.6	01-Sep-17	-	nd	-
MS2 9/17	Solfatara	mud pool	north part, mud with acicular	49.9-48.6	01-Sep-17	-	nd	-

			material and grains					
MS3 9/17	Solfatara	mud pool	Sulfur into the fracture determined by drying	49.9-48.6	01-Sep-17	-	nd	-
BG 9/17	Solfatara	Bocca Grande	Sulfur, abundant in mushy form	>87.5	01-Sep-17	Sulfur (shifted pattern)	nd	-
MS new 9/17	Solfatara	new pool	level lowering, mushy mud that is drying	63-70	01-Sep-17	Alunite, Pyrite, Alum-(Na), Kaolinite, Amorphous	nd	-
L1 S	Pisciarelli	L1 main vent	-	-	18-Sep-17	Sulfur	nd	-
L1 efflorescenza beije_sep rosso	Pisciarelli	L1 main vent	reddish from beije efflorescence	-	18-Sep-17	Alunogen (slightly shifted pattern)	nd	-
L1 efflorescenza beije_sep bianco	Pisciarelli	L1 main vent	white from the beije efflorescence	-	18-Sep-17	Alunogen	nd	-
PINT S	Pisciarelli	PINT	Acicular Sulfur	-	18-Sep-17	Sulfur	nd	-
L20 Camino	Pisciarelli	L20 high area	Sulfur as a crust	-	18-Sep-17	Sulfur, Alunite	nd	-
L20 camino mud + S	Pisciarelli	L20 high area	Sulfur patina on gray clay	94.2	18-Oct-17	Alunite, Sulfur, Amorphous	nd	-
L20 camino mud + S_S	Pisciarelli	L20 high area	Sulfur patina on gray clay	94.2	18-Oct-17	Pyrite, Alunite, Sulfur, Amorphous	nd	-
L20 camino efflorescenza	Pisciarelli	L20 high area	grayish-to-whitish neogenesis	41.5	18-Oct-17	Tschermigite	nd	-
L20 camino S patina	Pisciarelli	L20 high area	Sulfur encrustation, patina	-	18-Oct-17	Sulfur	nd	-
PINT rosso	Pisciarelli	PINT	red clay containing white rounded grain	90.5	18-Oct-17	Alunite, Hematite, Kaolinite, Sanidine	nd	-

PINT rosso_bianco	Pisciarelli	PINT	white rounded grain of the red clay above	90.5	18-Oct-17	Alunite, Kaolinite		nd	-
PINT S tozzo	Pisciarelli	PINT	Sulfur, blocky	88.9	18-Oct-17	Sulfur 01-078-1888		nd	-
PINT rosso palline bianche	Pisciarelli	PINT	white clay grains inside the red clay above	90.5	18-Oct-17	-		nd	-
MP	Pisciarelli	L3 - mud pool	mud at the west border	88.7	18-Oct-17	Alunite, Biotite, Illite, Clorite, Vermiculite, Pyrite, Sulfur, Sanidine, Amorphous		nd	-
MP_mud decantato	Pisciarelli	L3 - mud pool	mud decanted from water at the bubbling point	84	18-Oct-17	Alunite, Sulfur, Anorthoclase, Amorphous		nd	-
MP _evapo dendritici	Pisciarelli	L3 - mud pool	water at the centre, bubbling point, crystals from evaporation	84	18-Oct-17	Sulfur, Mascagnite, Alunite, Marialite, Oxybiotite, Amorphous		nd	start water sampling from pools
MP _evapo tozzi	Pisciarelli	L3 - mud pool	water at the centre, bubbling point, crystals from evaporation	84	18-Oct-17	Ammonium sulfate (mascagnite), Bormuscovite, Sulfur, Paramelaconite (CuO)		nd	-
L1 vent S cristallino	Pisciarelli	L1	Sulfur crystals from varios point of the wall	-	18-Oct-17	Sulfur (pattern 2283)		nd	-
L1 vent S cristallino_substr	Pisciarelli	L1	substratum of the Sulfur	-	18-Oct-17	Sulfur, Alunite, Pyrite		nd	-
L1 vent S patina	Pisciarelli	L1 vent	yellow patina	95.2	18-Oct-17	Sulfur		nd	-
L1 parete S	Pisciarelli	L1 wall, base	fine acicular crystals at the base	89.6	15-Nov-17	Sulfur		nd	-
L1 pareteEFF	Pisciarelli	L1 wall, upper part	soft white efflorescence	34.5	15-Nov-17	Alunogen, Alum-(K), Sulfur		nd	-

L1 pareteEFF_impurità	Pisciarelli	L1 wall, upper part	soft whitish efflorescence	34.5	15-Nov-17	Alunite (with Cr?), Alunogen	nd	-
L1 parete crosta	Pisciarelli	L1 wall, medial part	hard-to-friable white encrustation	37	15-Nov-17	Alum-(K), Alunite (likely with Cr?)	nd	-
L30 mud	Pisciarelli	L30	beije mud in a cm-wide hole filled by water	41.7	15-Nov-17	Alunite, Amorphous, bad pattern	nd	-
L3 acqua_decantata	Pisciarelli	L3 - mud pool	mud decanted from water at the bubbling point nearby L1	85	15-Nov-17	Sulfur, Alunite, Mascagnite, Biotite, Amorhous	nd	-
L3 acqua_evaporata	Pisciarelli	L3 - mud pool	water at the bubbling point nearby L1, crystals from evaporation	85	15-Nov-17	Mascagnite, Gypsum, Boromuscovite and other difficult to define	nd	-
L3 mud	Pisciarelli	L3 - mud pool	mud, nearby PEXT	87	15-Nov-17	Alunite, Pyrite, Feldspar, Sulfur, Illite, Amorphous, bad pattern	nd	-
L19 geiser	Pisciarelli	L19	gray mud nearby geiser and fine flowing water	90	15-Nov-17	Alunite, Pyrite, high Amorphous content. bad pattern low crystallinity	nd	-
L1 vent S_S	Piciarellli	L1 vent	sulfur at main fumarol	94.7	14-Dec-17	Sulfur	nd	-
L1 vent S film_all	Piciarellli	L1 vent	substratum of sulfur main, fumarol	94.7	14-Dec-17	Sulfur, Pyrite, Alunite, Amorphous	nd	-
L20 camino S	Piciarellli	L20	Sulfur	77.8	14-Dec-17	Illite, Sulfur, Alunite, Amorphous	nd	-
L20 crema	Piciarellli	L20	Cream-like	-	14-Dec-17	Alunite, Amorphous	nd	-
L30 mud	Piciarellli	L30	beije mud in a cm-wide hole filled by water	42.1	14-Dec-17	Alunite, Sulfur, Amorphous. bad pattern	nd	-
L3 acqua_decantato	Piciarellli	L3 - mud pool	mud decanted from water at	84.5	14-Dec-17	Sulfur, Alunite, Pyrite, Titanite, Amorphous	nd	-

			the bubbling point nearby L1					
L3 acqua_cristallizzato	Piciarellli	L3 - mud pool	water at the bubbling point nearby L1, crystals from evaporation	84.5	14-Dec-17	Mascagnite, Tschermigite, Letovicite, Mohrite, Biotite	nd	-
L3 mud MP	Piciarellli	L3 - mud pool	mud, nearby PEXT	77.4	14-Dec-17	Pyrite, Sulfur, Alunite, Sanidine, Amorphous, Illite?	nd	-
L19 Geiser mud	Piciarellli	L19	mud, between Geisers	-	14-Dec-17	Alunite, Sulfur, Plagioclase, Amorphous	nd	-
L19 Geiser marrone_all crosta	Piciarellli	L19	uppermost Geiser, bulk, brown crust	95.3	14-Dec-17	Alunite, Pyrite (greigite), Amorphous, Quartz?	nd	-
L19 Geiser marrone	Piciarellli	L19	uppermost Geiser, brown material from above sample	95.3	14-Dec-17	Alunite, Sanidine, Phlogopite, Amorphous	nd	-
L19 Geiser crema_whole	Piciarellli	L19	uppermost Geiser, cream-like, bulk	95.3	14-Dec-17	Alunite, Amorphous	nd	-
L19 Geiser crema_imp bianco	Piciarellli	L19	uppermost Geiser, cream-like, whitish from the above sample	95.3	14-Dec-17	Pyrite, Alunite, Amorphous	nd	-
Geiser bianco (anche un po' arancio)	Piciarellli	Geiser	Back wall, white	-	14-Dec-17	Alunite, Quartz, Amorphous	nd	-
Geiser arancione	Piciarellli	Geiser	wall toward L60, orange	-	14-Dec-17	Jarosite, Alunite, Amorphous	nd	-
Geiser rosso	Piciarellli	Geiser	nearby the main output, reddish	-	14-Dec-17	Jarosite, Alunite, Fe-hydroxides	nd	-
MP acqua polla =L3 acqua	Piciarellli	L3 - mud pool	grayish water, crystals from evaporation	85.4	18-Jan-18	Mascagnite, Letovicite	nd	-

MP mud	Piciarellli	L3 - mud pool	blackish mud	77.1	18-Jan-18	Alunite, Sulfur, Pyrite, Anorthoclase, Amorphous, illite	nd	-
L1 vent S	Piciarellli	L1 vent	crystallizing sulfur	94	18-Jan-18	Sulfur, Pyrite	nd	-
L1 ventparete S	Piciarellli	L1 wall	diffuse crystalline sulfur on the wall nearby the vent	89.9	18-Jan-18	Alunogen, Sulfur	nd	-
L1 parete verde	Piciarellli	L1 wall	greenish portions within whitish part	72.5	18-Jan-18	-	nd	-
PINT S_puro	Piciarellli	PINT	Blocky and denditric sulfur	93.4	18-Jan-18	Sulfur	nd	-
PINT S_bulk	Piciarellli	PINT	Blocky and denditric sulfur	93.4	18-Jan-18	Sulfur	nd	-
PINT rosa	Piciarellli	PINT	pinkish material	93.4	18-Jan-18	Feldspatoid? Very high abundance of Amorphous. bad pattern	nd	-
L20 vent mud	Piciarellli	L20	blackish-greenish mud on whitish material	95.8	18-Jan-18	Alunite, Pyrite, Amorphous	nd	-
L19 vent Geiser S	Piciarellli	L19 Geiser	blackish-greenish mud on whitish material	95.8	18-Jan-18	-	nd	-
L20 camino mud	Piciarellli	L20	dryied mud esfoliar	81	18-Jan-18	Alunite, Amorphous	nd	-
L70 S	Piciarellli	L70	Sulfur on chimney at the base of the collapsed slope	68	18-Jan-18	Sulfur	nd	-
L70 eff	Piciarellli	L70	efflorescence uppermost on the wall source of L70S	-	18-Jan-18	Alunogen, Tschermingite, Amorphous	nd	-

L60 Geiser acqua	Piciarellli	L60	limpid water from bubbling aquifer into a hole back to the Geiser, crystals from evaporation	93.6	18-Jan-18	Tschermingite, Gypsum		nd		-
L60 Geiser S	Piciarellli	L60	Sulfur within the hole above in which the acquifer is bubbling	-	18-Jan-18	Sulfur		nd		-
										-
MP acqua polla =L3 acqua	Piciarellli	L3 - mud pool	turbid, grayish water, crystals from evaporation	94.1	16-Feb-18	Tschermigite, Mascagnite		nd		-
MP	Piciarellli	L3 - mud pool	gray mud	74.1	16-Feb-18	Alunite, Sulfur, Pyrite, orthoclase, Illite, Amorphous		nd		-
L30 fiori	Piciarellli	L30	beije efflorescence nearby the cm-wide hole	40.7	16-Feb-18	Alunogen, Quartz		nd		-
L30 eff1	Piciarellli	L30	beije efflorescence on the wall nearby the cm-wide hole	40.7	16-Feb-18	Alunogen plus other but very complicated pattern		nd		-
L30 eff2	Piciarellli	L30	beije efflorescence on the wall nearby the cm-wide hole	40.7	16-Feb-18	-		nd		-
CIN1al_grigio	Cinofilo	CIN	uppermost part, gray portion in the whitish material	-	16-Feb-18	Pyrite, Sulfur, Sanidine, Amorphous		nd		-

CIN1al_bianco	Cinofilo	CIN	uppermost part, whitish material	-	16-Feb-18	Titanium oxide, Opal, Amorphous (high content)	nd	-
CIN2 crema	Cinofilo	CIN	uppermost part, cream-like whitish material	-	16-Feb-18	Titanium oxide (Al), Opal, Amorphous (high content)	nd	-
F1 CIN duro	Cinofilo	CIN	low hot site, hard encrustation	96.2	16-Feb-18	Alunogen, Zeolites, Sanidine	nd	-
F1 CIN S	Cinofilo	CIN	low hot site, yellow sulfur	96.2	16-Feb-18	Sulfur	nd	-
F1 CIN2 ara	Cinofilo	CIN	low hot site, orange concrection	96.2	16-Feb-18	Jarosite, Alunite	nd	-
CIN1 b eff arancione	Cinofilo	CIN	low hot site, orange concrection, at the base	53.6	16-Feb-18	Sanidine, Gypsum, Clay interlayer (illite/Montmorillonite)	nd	-
CIN1 b eff bianca	Cinofilo	CIN	low hot site, orange concrection, at the top	53.6	16-Feb-18	Tamarugite, Jarosite, Hexahydrite, Picropharmacolite, Zaherite	nd	-
MP acqua polla =L3 acqua	Piciarellli	L3 - mud pool	turbid, greenish water, crystals from evaporation	84.3	16-Mar-18	Mascagnite, Tschermigite, Letovicite, Muscovite, Sulfur plus other but complicated	nd	-
MP	Piciarellli	L3 - mud pool	gray mud	84.3	16-Mar-18	Alunite, Amorphous, Pyrite, Sanidine, Illite	nd	-
PINT S	Piciarellli	PINT	denditric, encrustated sulfur	94.4	16-Mar-18	Sulfur pure	nd	-
L60 acqua	Piciarellli	L60	clean water in the hole back to the Geiser, deepened aquifer level, crystals from evaporation	92.2	16-Mar-18	Alunogen, Manganese thiocyanate, Akuammine, Aluminium Sulfate	nd	-

L60 S	Piciarellli	L60	Sulfur at the deepened aquifer level in the hole back to the Geiser above	92.2	16-Mar-18	Sulfur	nd	-
L60 S_bianco	Piciarellli	L60	white portion at the deepened aquifer level in the hole back to the Geiser above	92.2	16-Mar-18	Amorphous, Alunite, Sulfur	nd	-
L20 rugine_bianco	Piciarellli	L20	orange-reddish portion on whitish substratum	-	16-Mar-18	Alunite, Amorphous, Pyrite, Illite/Montmorillonite?	nd	-
L20 rugine_rosa	Piciarellli	parte alta a sud polla	orange-to-reddish portions of previous sample	-	16-Mar-18	Amorphous, Alunite, Montmorillonite	nd	-
L19 vent N S	Piciarellli	L19	substratum for S, south of L60	-	16-Mar-18	Sulfur, low abundant Alunite	nd	-
L19 vent N S_substrato	Piciarellli	L19	substratum for S, south of L60	-	16-Mar-18	Sulfur, Amorphous, Alunite, Feldspar?	nd	-
Cam Caliro	Piciarellli	Geiser	acicular whitish crystals forming an efflorescence at the surface	-	01-Apr-18	Alunogen	nd	-
L3 water pool	Piciarellli	L3 - mud pool	water	84.6	22-May-18	Alunogen, Mascagnite	nd	-
MP	Piciarellli	L3 - mud pool	gray mud	84.6	22-May-18	Alunite, Sanidine, Pyrite, Sulfur, Amorphous	nd	-
Viadotto	Piciarellli	Viadotto	gray, stratified mud	40.8	22-May-18	Alunite, Sanidine, Pyrite, Sulfur, Amorphous	nd	-
L30 mud	Piciarellli	L30	beije, humid mud in a cm-wide hole	71	22-May-18	Alunite, Amorphous	nd	-

L1 vent S	Pisciarelli	L1 vent	low abundance of Sulfur on the blackish substratum	95.1	22-May-18	Sulfur		nd	-
PINT S	Piciarellli	PINT	dendritic encrustated sulfur	94.8	22-May-18	Sulfur		nd	-
L20 new vent mud	Piciarellli	L20	gray mud around the vent, reddish at the surface	94.9	22-May-18	Alunite, Pyrite, Clay (Illite/Montmorillonite interlayer?)		nd	-
L20 eff beije	Piciarellli	L20, on the east	beije efflorescence, flower-like	-	22-May-18	Alum-(Na), Letovicite		nd	-
L20 eff bianca	Piciarellli	L20, on the east	white efflorescence, flower-like	-	22-May-18	Tamarugite, Feldspar		nd	-
L19 N vent S	Piciarellli	L19	sulfur on greenish-whitish wall	-	22-May-18	Sulfur		nd	-
L60 S	Piciarellli	a monte del Geiser	Sulfur at the water level of the hole above	93.9	22-May-18	Sulfur		nd	-
Geiser ara	Piciarellli	intorno al Geiser	orange exfoliating encrustation		22-May-18	Tschermigite, Jarosite, Amorphous		nd	-
MP	Piciarellli	L3 - mud pool	blackish mud	83.8	26-Jun-18	Alunite, Sanidine, Pyrite, Sulfur, Amorphous		nd	-
MP acqua polla =L3 acqua	Piciarellli	L3 - mud pool	blackish turbid water, crystals from evaporation	83.8	26-Jun-18	Mascagnite, Gypsum, Zeolites		nd	-
MP acqua polla =L3 acqua con residuo	Piciarellli	L3 - mud pool	blackish turbid water, crystals from evaporation	83.8	26-Jun-18	Mascagnite, Gypsum, Zeolites		nd	-

L1-L3 eff suolo	Piciarellli	between pool and L1	orange efflorescence at the soil	-	26-Jun-18	Mascagnite, Zeolite, Letovicite	nd	-
L30 eff	Piciarellli	L30, nearby hole	whitish flower-like efflorescence newrby greenish part	-	26-Jun-18	Alunogen, Fe-phosphate? and/or Jarosite	nd	-
L30 eff_blocchetto	Piciarellli	L30, nearby hole	white flower on the greenish portions	-	26-Jun-18	Alunite, Alunogen, Amorphous	nd	-
L30-L1 eff	Pisciarelli	between L30 and L1	soft, whitish	-	26-Jun-18	Alunogen, Chabazite	nd	-
L100 base	Piciarellli	L100, south west of L60	dried mushy efflorescence, at the base of the wall	-	26-Jun-18	Alunite, Alunogen	nd	-
L100 granu	Piciarellli	L100, south west of L60	dried granular efflorescence, medial on the wall	-	26-Jun-18	Alunite, Alunogen	nd	-
L100 eff	Piciarellli	L100, south west of L60	friable encrustation on the granular efflorescence	-	26-Jun-18	Alunite, Alunogen	nd	-
L100 zucc	Piciarellli	L100, south west of L60	sugar-like efflorescence, topmost	-	26-Jun-18	Alunogen	nd	-
MP	Piciarellli	L3 - mud pool	mud	81.6	18-Jul-18	Alunite, Sanidine, Pyrite, Sulfur, OxyBiotite/Illite, Amorphous	nd	-
MP acqua polla =L3 acqua	Piciarellli	L3 - mud pool	water, crystals from evaporation	81.6	18-Jul-18	Mascagnite, Sulfur, Biotite	nd	-
L3 schiuma	Piciarellli	L3 - mud pool	foam at the pool limit	81.6	18-Jul-18	Sulfur, Alunite, Melanterite	nd	-

L1S	Piciarellli	L1 parete	low abundant sulfur	-	18-Jul-18	Sulfur		nd		-
L71S	Piciarellli	L71	low abundant sulfur along the collapsed and mined wall	94.1	18-Jul-18	Sulfur		nd		-
PEXT S	Piciarellli	PEXT	dendritic hair-like sulfur	94.6	18-Jul-18	Sulfur		nd		-
PINT S	Piciarellli	PINT	dendritic hair-like encrustation of sulfur	95	18-Jul-18	Sulfur		nd		-
L20M ara	Pisciarelli	top L20	orange wall along the uppermost pathway	-	18-Jul-18	Tschermigite, Illite/Montmorillonite, Amorphous (low abundance)		nd		-
L60 S	Piciarellli	L60	deepening water level in the hole back to Geiser	-	18-Jul-18	Sulfur		nd		-
L60b acqua	Piciarellli	L60 other	bubbling water between L60 and geiser, crystals from evaporation	-	18-Jul-18	any crystallization		nd		-
MP-viadotto	Piciarellli	between L1, viadotto, pool border	mushy blackish mud	55.3	26-Sep-18	Alunite, Sulfur, Amorphous (low abundance)		3.9-4.5		-
L3 acqua	Piciarellli	L3 - mud pool	water nearby PEXT, crystals from evaporation	94.3	26-Sep-18	Illite/Montmorillonite, Ammonium K sulfate		4.8		-
MP-L3	Piciarellli	L3 - mud pool	black, granular mud	94.3	26-Sep-18	Alunite, Sanidine, Pyrite, Sulfur, HydroBiotite/Illite, Amorphous		4.8		-
L3 Geiser	Piciarellli	L3 - mud pool	water nearby the Geiser, crystals	80.1	26-Sep-18	Mascagnite, Koktaite?, Sulfur		5.2		-

			from evaporation					
L60 S	Piciarellli	L60	deepening water level in the hole back to Geiser	93.9	26-Sep-18	Sulfur	1.6	-
L60 acqua	Piciarellli	L60 other	bubbling water	93.9	26-Sep-18	-	1.6	-
L1vent nero	Piciarellli	L1 vent	low abundant sulfur	95.8	26-Sep-18	Voltaite, Coquimbite, Pyrite	1.3	-
L1 base S	Piciarellli	L1	yellow sulfur at the wall base	-	26-Sep-18	Sulfur	nd	-
L1 parete S	Piciarellli	L1	pale yellow sulfur along the wall	-	26-Sep-18	Sulfur	nd	-
L1 bianco zucc	Piciarellli	L1	sugar-like along the wall	-	26-Sep-18	Alunogen, Alum-(K)	nd	-
PINT S	Piciarellli	PINT	dendritic, encrustated, hair-like sulfur	89.1	26-Sep-18	Sulfur	nd	-
BG	Solfatara	Bocca Grande	strong yellowish encrustation	-	26-Sep-18	Ammonium chloride, Arsenic sulfide (Realgar)	nd	-
BG	Solfatara	Bocca Grande	strong yellowish encrustation	-	26-Sep-18	Ammonium chloride, Arsenic sulfide (Realgar)	nd	-
BG	Solfatara	Bocca Grande	strong yellowish encrustation	-	26-Sep-18	Ammonium chloride, Arsenic sulfide (Realgar)	nd	-
L60b	Piciarellli	L60 other	bubbling milky water, crystals from evaporation	94	30-Oct-18	Potassium Ammonium Aluminum Sulfate Hydrate	1-2	-
L60	Piciarellli	L60 other	milky water, deepened aquifer level, crystals from evaporation	91.8	30-Oct-18	no sample	1-2	-
Fratturina	Piciarellli	between L30-L1	collected spray from a cm-long fracture, crystals	95.6	30-Oct-18	Mascagnite	7	-

			from evaporation							
MP	Piciarellli	L3 - mud pool	gray-black mud with up to cm-sized components	91.2	30-Oct-18	Alunite, Sanidine, Pyrite, Sulfur, HydroBiotite/Illite, Amorphous		5		-
L3 acqua	Piciarellli	L3 - mud pool	turbid water, crystals from evaporation	90.5	30-Oct-18	Mascagnite, Sulfur, Clay mineral		5		-
L1 vent	Piciarellli	L1 vent	gray-black without sulfur	95	30-Oct-18	Pyrite, Alunite, HydroBiotite/Illite, Amorphous		-		-
L1 S	Piciarellli	L1 base	sulfur at the wall base	-	30-Oct-18	Sulfur		-		-
MP viadotto	Piciarellli	viadotto	mud with water abundance	-	30-Oct-18	Alunite, Sanidine, Sulfur, Amorphous, Illite?		-		-
L20 camino	Piciarellli	L20	gray mud	91.8	30-Oct-18	Alunite, Pyrite, Amorphous		-		-
L19	Piciarellli	L19	translucid black mud with orange and white crystals	94.8	30-Oct-18	Pyrite, Alunite, Amorphous (low abundance)		-		-
L100S	Piciarellli	L100	sulfur	92.6	30-Oct-18	Sulfur		-		-
L100 nero	Piciarellli	L100	substratum of sulfur	92.6	30-Oct-18	Sulfur, Quartz, Amorphous		-		-
L70	Piciarellli	L70	black material with sulfur	93.3	30-Oct-18	-		-		-
Stufe Pozzo1	Baia	Stufe di Nerone	water from well, crystals from evaporation	76	31-Oct-18	Halite		7.06		-
Stufe spring	Baia	Stufe di Nerone	water springs, crystals from evaporation	78.6	31-Oct-18	Halite		7		-

L60b acqua	Piciarellli	L60 other	bubbling milky water between L60 and geiser, crystals from evaporation	92.6	29-Nov-18	Ammonium sulafte, Alum-(K)		-	-
L60 mud	Piciarellli	L60 wall on the back	plastered grayish mud	-	29-Nov-18	Alunite, Orthoclase, Pyrite, Amorphous		-	-
L3 acqua	Piciarellli	L3 - mud pool	milky grayish water, crystals from evaporation	85.7	29-Nov-18	Mascagnite, Koktaite (sulfate calcium ammonium hydrate)		-	-
MP	Piciarellli	L3 - mud pool	mud with cm-sized components	85.7	29-Nov-18	Alunite, Sulfur, Hydrobiotite/Illite, Orthoclase, Pyrite, Amorphous		-	-
PEXT S	Piciarellli	PEXT	S encrustation and crystals	93.7	29-Nov-18	Sulfur		-	-
L1 wext	Piciarellli	L1, external side, proxy to L30	efflorescence and encrustation through a fracture of the white wall	-	17-Jan-19	Alunite, Alunogen		-	-
G19 fango ess	Piciarellli	G19, mud vent	dried gray-greenish mud from a vent opened nearby the Geiser and the pool	91.5	17-Jan-19	Alunite, Amorphous		-	-
G19 fango fluido	Piciarellli	G19, mud vent	gray fluid mud coexisting with the above	91.5	17-Jan-19	Alunite, Mascagnite, Amorphous.		-	-
G19-S	Piciarellli	G19, mud vent	yellowish encrustation on the mud above	91.5	17-Jan-19	Sulfur, Alunite		-	-
G19_ara	Piciarellli	G19, mud vent	brow-orange encrustation on the mud above	91.5	17-Jan-19	Clairite, Mohrite		-	-

G19_eff bianca	Piciarellli	G19, mud vent	whitish encrustation coexisting with the G19 materials above	91.5	17-Jan-19	Alunite, Jarosite?, Amorphous		-	-
MP	Piciarellli	L3 - mud pool	decanted mud sample from the east side of the pool	88.6	17-Jan-19	Alunite, Sulfur, Pyrite, Orthoclase, Amorphous		-	-
L3	Piciarellli	L3 - mud pool	water from the east side of the pool, crystals from evaporation	88.6	17-Jan-19	Mascagnite, Gypsum, Koktaite		-	-
PEXT_S	Piciarellli	PEXT	sulfur	94.6	17-Jan-19	Sulfur		-	-
G19_aranew	Piciarellli	G19, mud vent	orange-brownish encrustation	84.1	24-Jan-19	Mascagnite, alunogen, Zaherite, Amorphous.		-	-
G19_red	Piciarellli	G19, mud vent	reddish encrustation	84.1	24-Jan-19	Titanium oxide, Amorphous.		-	-
L100 ara	Piciarellli	L100	orange-brownish encrustation, southeast L60	-	24-Jan-19	Alunogen, Voltaite, Coquimbite, Zaherite, Gypsum.		-	-
L60-polla1	Piciarellli	L60	whitish substratum for algae, wall of the hole, top part	40	06-Feb-19	Alunite, Amorphous		-	-
L60-polla2	Piciarellli	L60	whitish substratum for algae, wall of the hole, lowermost part	40	06-Feb-19	Natroalunite, Opal, Amorphous		-	-
L1wall incrostazione	Piciarellli	L1 wall	fissure with algae on which granular encrustation occurs	34	06-Feb-19	Alum-(K)		-	-

PEXT_parte verde	Piciarellli	PEXT	brownish film on whitish substratum with algae, greeenish part	34	06-Feb-19	Potassium Ammonium Aluminum Sulfate Hydrate, Alunite, Amorphous	-	-
PEXT_parte marroncina	Piciarellli	PEXT	brownish film on whitish substratum with algae, brown part	34	06-Feb-19	Alunite, Sulfur, Amorphous.	-	-
PEXT_parte biancastra	Piciarellli	PEXT	brownish film on whitish substratum with algae, white part	34	06-Feb-19	Alunite, Amorphous.	-	-
MP	Piciarellli	L3 - mud pool	mud decanted water, east side of the pool	88	06-Feb-19	Alunite, Sulfur, Pyrite, Orthoclase, Amorphous, Illite	-	-
L3	Piciarellli	L3 - mud pool	water, east side of the pool, crystals from evaporation	88	06-Feb-19	Mascagnite, Illite	-	-
G19	Piciarellli	G19, mud vent	encrustation	-	06-Feb-19	Alunite, Mascagnite, Voltaite, Zaherite, Amorphous	-	-
L60b acqua	Piciarellli	L60	water	-	04-Apr-19	Mascagnite, Gypsum	-	-
L60 acqua	Piciarellli	L60	water	93.6	04-Apr-19	-	-	-
MP	Piciarellli	L3 – mud pool	mud decanted water,	87.5	04-Apr-19	Alunite, Pyrite, K-feldspar, Amorphous	-	-
L3	Piciarellli	L3 - mud pool	water, of the pool, crystals from evaporation	87.5	04-Apr-19	Mascagnite, Alunogen	-	-
MS new	Solfatara	new pool	mushy mud	91	04-Apr-19	Alunite, Kaolinite, Pyrite, Amorphous	-	-
MS	Solfatara	La Fangaia	mud	-	04-Apr-19	Alunite, Amorphous	-	-
BN	Solfatara	Bocca Nuova	encrustation	136	04-Apr-19	Salammoniac	-	-

BG	Solfatara	Bocca Grande	encrustation	141	04-Apr-19	Mascagnite, Salammoniac	-	-

Table S2 – Vibration modes and related tentative assignment of functional groups, and mineral attribution for selected samples by DRIFT-FTIR investigations. Alu = alunite, Clay = illite/montmorillonite, Masc = NH_4 - bearing sulfates, am = amorphous, Kao = kaolinite, KAl = alum - (K). ?, uncertain attribution. Note: assignments and attributions are based on mineralogy derived by XRDP study and corroborated by EDS-BSEM analyses. Further details in this supplement.

SOLFATARA MUDS					**PISCIARELLI MUDS**		
5/6/16	**24/7/17**	**1/9/17**	**Tentative Assignment**	**PH**	**6 /16**	**15/11/ 17**	**14/12/ 17**
4603	4606	h	Al-OH	Alu	4608h	-	4593h
4529	4528	x	Al-OH		4518x	-	-
-	4311	x	Mg-OH	Clay?	-	-	-
3973x	3975p	3980x		Alu	3971x	3976x	3973x
-	-	-		Clay	3629	3622	3622
-	3692p	-			-	-	-
3587h	3620x	h	ν1OH?	Clay?	-	-	-
3505p	3506p	3506p	ν1OH	Alu	3506p	3510p	3512p
3486p	3486p	3484p	ν1OH	Alu	3483p	3486p	3486p
3284h	3318h	3275h	ν1OH?	Clay?	3268h	-	-
-	-	-			-	3333h	3322h
2338p	2339p	2337p			2340p	2338p	2338p
2287	2291x	2289x	$2\nu_3SO_4$	Alu	2285	-	-
-	-	-			-	2289	-
2220	2223x	x	$2\nu_3SO_4$	Alu	2225h	-	-
2176p	2176p	2176p	$2\nu_3SO_4$	Alu	2175x	2178x	2176x
2119p	2117p	2116p	$2\nu_3SO_4$	Alu	2112p	2118x	2117x
1990p	1981x	1988p		Opal?	1997h	1985h	1980h
1870p	1872p	1873p		Opal?	1868p	1870p	1869p
1635p	1629p	1628p	δHOH		1630p	1637p	1629p
1436x	1431p	1432x	$\nu 4NH_4$	Masc?	1431-00	1437p	1434p
1215	1219x	1215h	Si-O	Clay, am?	1216x	1216	1219
1159	1158x	1158x			1158	-	1156
1102p	1101p	1102p	ν_3SO_4	Alu	1095p	1099p	1099p
1027p	1028p	1028p	ν_1SO_4	Alu	1027p	1028p	1028p
949p	943p	947p	AlAlOH	Clay?	-	-	-
-	-	-	AlAlOH	Clay?	929h	934h	936h

SOLFATARA NEW HOLE				
MSnew 5/17	**MSnew 7/17**	**MSnew 9/17**	**Tentative assignment**	**Phase**
4605x	4608	4613x+4586	Al-OH	Alu
4523p	4525x	4525p	Al-OH	Kao
4308?	4307?	4307x	Mg-OH	-
3976p	3980p	3976p		Alu
3694p	3695p	3695p	ν1OH	Kao
3668p	3666p	3667p	ν1OH	Kao
3652p	3651p	3651p	ν1OH	Kao
3620p	3620p	3620p	ν1OH	Kao
3510x	3510p	3509x	ν1OH	Alu
3483p	3483p	3483p	ν1OH	Alu
3354x	-	-	νOH	KAl
3006x	-	-	νOH	KAl
3410-2650H	3418-2650H	3410-2650H	νOH	-
2460h	-	-	νOH	KAl
2338x	2338p	2338x	-	-
2290x	2291p	2288x	$2\nu_3SO_4$	Alu
2221x	2228x	2222x	$2\nu_3SO_4$	Alu
2176x	2177p	2176x	$2\nu_3SO_4$	Alu
2115x	2115p	2116x	$2\nu_3SO_4$	Alu
1994hx	1995hx	1991hx		Opal?
1875p	1870p	1874p		Opal?
1630p	1637p	1631p	δHOH	
1435p	1431p	1431p	ν_4NH_4	Masc?
1228p	1229p	1231p	$\nu 3OH + \nu_3SO_4$	Alu, KAl
1156x	1158x	1158x		
1095p	1097p	1092p	ν_3SO_4, Si-O	Alu, KAl, Kao
1026p	1029p	1028p	ν_1SO_4, Si-O	Alu, Kao

-	871p	-			-	-	-
-	850p	-		S?	-	-	-
798p	801h	801p	SiO	am, clay	796p	796p	793p
682p	685p	686p	ν_4SO_4	Alu	680p	684p	683p
634p	636p	632p	ν_4SO_4	Alu	634p	631p	629p
604p	602p	604p	γOH	Clay	601p	603p	602p
-	576x	-					
526x	526	527p	Al-O-Si	Clay	-	524	526
470x	469p	467p	Si-O-Si	S? Clay?	-	469	470
-	-	-			-	-	-

1008x	1010x	1012x	Si-O	Opal? Kao
938x	939p	938x	OH	Kao
912p	916p	915p	OH	Kao
795p	794p	795p	Si-O	Opal? Kao
685p	688p	684p	Al-O, ν_4SO_4	Kao, Al, KAl
631p	635p	631p	Si-O, ν_4SO_4	Kao, Al
601p	604p	601p	δOH	Kao
532p	546-529	540p	Al-O-Si	Kao, clay
474p	473p	481-467p	Si-O-Si	Kao, clay
433p	435p	432p	Si-O	Kao

Table S3 – Selected whole-rock geochemistry of multi-phases materials sampled at different locations (i.e., sample name as in Fig. 1) within the Pisciarelli and Solfatara areas and at different times. MDL indicates the detection limit for major, trace, C and S contents.

Name	**Method**	**MDL**	**MPS0517**	**MP**	**MSnew**	**MS**	**L20camino**	**L1 beije**	**MS new**	**MS2**	**MP**	**L19Geiser**	**BG**	**L3 MP**
Sampling Date			31.5.17	29.6.17	29.6.17	29.6.17	18.9.17	18.9.17	1.9.17	1.9.17	15.11.17	14.12.17	20.9.16	14.12.14
SiO_2	ICP-ES	0.01%	49.43	38.05	49.27	49.59	15.73	3.09	48.71	72.52	59.78	63.33	80.56	56.32
Al_2O_3	ICP-ES	0.01%	16.2	10.01	16.04	4.97	2.35	14.67	16.72	3.43	10.38	11.32	1.29	11.85
Fe_2O_3	ICP-ES	0.04%	4.02	2.35	3.88	0.29	0.09	3.11	3.79	0.26	2.31	0.78	0.14	3.2
MgO	ICP-ES	0.01%	0.02	0.08	0.02	0.03	<0.01	0.01	0.02	0.04	0.15	0.05	0.04	0.16
CaO	ICP-ES	0.01%	0.08	0.14	0.08	0.08	0.02	0.05	0.07	0.09	0.25	0.03	0.07	0.3
Na_2O	ICP-ES	0.01%	0.18	0.24	0.18	0.13	0.03	0.03	0.2	0.11	0.34	0.07	0.02	0.42
K_2O	ICP-ES	0.01%	3.27	2.85	3.32	1.4	0.62	2.84	3.45	0.93	3.34	3.08	0.18	3.9
TiO_2	ICP-ES	0.01%	0.51	0.35	0.52	0.73	0.34	0.07	0.5	0.71	0.52	0.66	2.35	0.49
P_2O_5	ICP-ES	0.01%	0.21	0.1	0.21	0.09	0.03	0.03	0.21	0.07	0.11	0.07	0.03	0.12
MnO	ICP-ES	0.01%	<0.01	<0.01	<0.01	<0.01	<0.01	<0.01	<0.01	<0.01	<0.01	<0.01	<0.01	<0.01
Cr_2O_3	ICP-ES	0.00%	0.003	<0.002	0.004	<0.002	<0.002	<0.002	0.003	<0.002	0.002	<0.002	0.003	<0.002
Ba	ICP-ES	1 ppm	966	952	975	817	401	69	918	677	1611	967	4261	1789
Ni	ICP-ES	20 ppm	<20	<20	<20	<20	<20	<20	<20	<20	<20	<20	<20	<20
Sc	ICP-ES	1 ppm	4	3	4	3	<1	2	4	2	3	4	2	4
LOI	ICP-ES	-5.10%	25.8	45.6	26.2	42.5	80.7	76	26	21.7	22.5	20.4	14.7	22.9
Sum	ICP-ES	0.01%	99.8	99.89	99.8	99.89	99.96	99.94	99.8	99.9	99.87	99.86	99.8	99.86
Be	ICP-MS	1 ppm	<1	1	<1	1	<1	<1	2	<1	4	5	2	5
Co	ICP-MS	0.2 ppm	10.6	4.2	8.3	0.7	<0.2	1.4	9.3	0.6	3.4	0.4	0.6	5.7
Cs	ICP-MS	0.1 ppm	4.6	6.4	4.6	4.5	3.3	1.1	4.3	7.3	9.8	23.4	14.5	9.3
Ga	ICP-MS	0.5 ppm	22.5	10.2	23.8	6.9	2.1	9.5	22.7	4.2	9.1	15.6	0.8	10.7
Hf	ICP-MS	0.1 ppm	8.8	5.1	8.6	10.2	3.3	0.8	8	11.2	6.6	9.6	11	6.2
Nb	ICP-MS	0.1 ppm	44	24.6	42.6	64.7	21.9	1.9	40.8	66.5	38	61.2	156.1	34.9
Rb	ICP-MS	0.1 ppm	41.5	54.8	39.5	26.5	11.4	22.6	45.9	29.5	73	75.8	26.9	83.7
Sn	ICP-MS	1 ppm	4	3	4	6	3	<1	4	5	3	4	20	3
Sr	ICP-MS	0.5 ppm	654.1	333.8	649.5	159.9	76.1	253.5	650.5	106.4	375.2	275	80.4	449.4
Ta	ICP-MS	0.1 ppm	2.3	1.3	2.3	3.2	1	0.1	2.3	3.3	2	3.1	7.6	1.9

Th	ICP-MS	0.2 ppm	26.9	13	25.1	13.2	5.5	6.7	25.3	12.7	15.5	24.5	8.4	16.3
U	ICP-MS	0.1 ppm	10.4	5.3	9.7	6.6	2.1	0.7	9.5	7.3	6.3	13.8	7.2	6.2
V	ICP-MS	8 ppm	110	58	102	35	16	21	106	24	59	72	54	65
W	ICP-MS	0.5 ppm	5.4	2.4	4.8	7	2.5	<0.5	4.3	8.1	4.8	5.1	18.7	3.9
Zr	ICP-MS	0.1 ppm	406	217.4	390.5	447.8	136	32.5	373.5	490.4	291.6	444.7	497.9	278.6
Y	ICP-MS	0.1 ppm	5.5	4.6	5.5	4.4	1.3	0.5	5.4	4.5	6	3.7	7.8	6.6
La	ICP-MS	0.1 ppm	74.8	31.6	69.6	24.1	12.3	24.3	71.7	16.8	37.2	46.2	11.2	40.9
Ce	ICP-MS	0.1 ppm	123.4	50.4	116.2	36.5	20.2	35	125.1	27.5	57.9	70.7	9.8	65.3
Pr	ICP-MS	0.02 ppm	12.05	4.71	11.17	3.45	1.76	2.29	12.08	2.62	5.53	5.22	0.86	5.94
Nd	ICP-MS	0.3 ppm	38.9	13.9	36.8	11.1	4.9	4	37.5	9.3	17.4	11.9	3.3	19.3
Sm	ICP-MS	0.05 ppm	5.37	2.14	5.18	1.82	0.51	0.54	5.33	1.5	2.48	1.15	0.78	2.59
Eu	ICP-MS	0.02 ppm	1.01	0.48	0.93	0.32	0.12	0.1	1.06	0.31	0.55	0.33	0.11	0.64
Gd	ICP-MS	0.05 ppm	3.1	1.44	2.96	1.15	0.39	0.25	3.15	1.04	1.64	0.94	0.97	1.75
Tb	ICP-MS	0.01 ppm	0.37	0.18	0.33	0.15	0.05	0.03	0.35	0.15	0.23	0.14	0.17	0.24
Dy	ICP-MS	0.05 ppm	1.4	0.93	1.33	0.77	0.27	0.16	1.47	0.86	1.14	0.75	1.11	1.18
Ho	ICP-MS	0.02 ppm	0.21	0.17	0.2	0.17	0.05	0.02	0.19	0.18	0.22	0.15	0.26	0.26
Er	ICP-MS	0.03 ppm	0.54	0.49	0.5	0.52	0.19	0.05	0.55	0.52	0.61	0.47	0.86	0.7
Tm	ICP-MS	0.01 ppm	0.08	0.07	0.07	0.07	0.02	<0.01	0.08	0.08	0.09	0.05	0.15	0.11
Yb	ICP-MS	0.05 ppm	0.6	0.59	0.64	0.61	0.19	0.08	0.61	0.58	0.68	0.39	0.93	0.7
Lu	ICP-MS	0.01 ppm	0.09	0.08	0.08	0.08	0.03	<0.01	0.09	0.1	0.11	0.07	0.15	0.11
TOT/C	LECO	0.02%	0.14	0.14	0.16	0.58	0.25	0.09	0.14	1.25	0.21	0.14	0.46	0.15
TOT/S	LECO	0.02%	8.75	31.12	8.42	24.9	>50.00	16.52	8.8	10.56	10.62	4.6	2.03	11.59
Mo	ICP-MS	0.1 ppm	2.8	0.9	3.1	1.8	0.4	0.9	2.3	1.5	1.3	1.3	1.2	1.2
Cu	ICP-MS	0.1 ppm	12.1	9.9	16.6	16.9	1.5	2.5	13.7	11.5	7.9	6	4.9	10.6
Pb	ICP-MS	0.1 ppm	20.9	14.8	20.3	12.9	3.9	12.7	18.1	13.4	19.9	38.4	15.9	20.1
Zn	ICP-MS	1 ppm	8	14	11	4	4	4	11	6	14	7	32	13

Ni	ICP-MS	0.1 ppm	7.8	2.8	8.6	0.2	0.3	0.8	9.1	0.7	2.6	1.3	0	3.1
As	ICP-MS	0.5 ppm	63.2	9.5	69.7	36.4	<0.5	2.9	69.6	25.6	10.9	0.9	6806.6	12.9
Cd	ICP-MS	0.1 ppm	<0.1	<0.1	<0.1	0.1	<0.1	<0.1	0.3	<0.1	<0.1	<0.1	0.2	<0.1
Sb	ICP-MS	0.1 ppm	19.9	0.2	11.7	3.5	0.1	<0.1	15.2	3.5	0.2	0.2	6	0.3
Bi	ICP-MS	0.1 ppm	0.5	0.3	0.7	1.2	0.1	0.3	0.5	1	0.2	0.1	0	0.2
Ag	ICP-MS	0.1 ppm	0.3	<0.1	<0.1	0.1	<0.1	<0.1	<0.1	<0.1	<0.1	<0.1	0.1	<0.1
Au	ICP-MS	0.5 ppb	12.1	<0.5	4.4	<0.5	<0.5	1.4	0.8	4.4	0.6	1.3	334.3	0.8
Hg	ICP-MS	0.01 ppm	50	41.95	>50.00	>50.00	12.75	2.9	>50.00	42.67	24.98	15.28	50	33.86
Tl	ICP-MS	0.1 ppm	2.1	1.5	2.3	0.3	<0.1	0.7	2	0.2	1.1	<0.1	0	1.7
Se	ICP-MS	0.5 ppm	<0.5	0.8	1.1	1.1	<0.5	<0.5	0.8	<0.5	<0.5	<0.5	<0.5	<0.5

Supplementary materials

1. Notes on XRDP and FT-IR techniques and spectra

In this work more than 350 samples collected at the solfataric area of the Campi Flegrei caldera, have been examined through X-Ray Powder Diffraction (XRDP). The interpretation of XRDP spectra, corroborated by Electron Microscopy (EDS-BSEM), provided the mineral dataset results. Selected samples have been further investigated through Diffuse Fourier Infrared Spectroscopy (DRIFT-FTIR) with the aim to explore eventual advantage of the technique on our mixtures and the suitability for detection of low abundant phases. Analytical techniques are in the Appendix.

Identification of phases has been obtained through the PANalytical software HighScore version 3.0e, considering the goodness of fit between the XRDP pattern of the unknown sample and those in the JCPDS PDF-2 database. Table S1 lists all the samples and the mineral dataset for the 350 samples representative of the period between 2012 and April 2019. Figure S1 displays representative XRDP spectra obtained on different samples and the peaks intensity of the identified phases. Each panel allows appreciating the comparable patterns obtained from different samples collected at the same sites. In particular, the panels S1a,b show the well-defined XRDP traces obtained on exsiccated water pool samples. The remaining panels illustrate the clays attribution to illite (S1d), kaolinite (S1e) and montmorillonite (S1f) in muds. The clays are usually present in low abundance in the analyzed samples; the La Fangaia muds (Fig. S1c) are the poorest of clays. The presence of the different clay minerals (i.e. illite, montmorillonite and kaolinite) has been established in consideration of the specific reflection lines. Furthermore, although the overlapping X-ray signals from associated clay mineral and amorphous phases, the traces of the intensity peaks in the interval between 20 ° and 40° 2θ degree suggest a dominance of well-ordered kaolinite (or kaolinite with low defect) in the Solfatara new pool (S1e).

Samples for which the mineral assemblage was preliminary identified by XRDP investigation give reproducible DRIFT-FT-IR spectra (see Fig. S2). Here, we show that the obtained DRIFT-FT-IR spectra can provide interesting information and major details will be obtained in the future if analyzing separated minerals. As matter of fact, we have examined the infrared spectra and we have identified some bands reported in the literature for the identified crystals (Table S2).

The various muds are complex mixtures derived by different mineral assemblages (Table S1, Fig. S1c,d,e,f). These muds always include alunite and it is possible recognizing clear infrared signals in the OH-stretching region attributable to that phase. Alunite produces the major band at 3483 cm^{-1} coupled with the smaller one at ca. 3513 cm^{-1} (Fig. S2c,d,e) described in the literature (Clark et al., 1990), also in our relatively complex muddy mixtures. On this basis, when the FT-IR spectra obtained from our muds are compared with those in the USGS database (Clark et al., 2007), other infrared signals of alunite can be revealed (Table S2): i) the peculiar shape of the FT-IR patterns between ca. 2290 and 2110 cm^{-1} with four consecutive bands can be associated with the $2\nu_3SO_4$ and ii) the band at ca. 1097-1100 cm^{-1} of ν_3SO_4. The band at ca. 1025 cm^{-1} that coupled with this later (Toumi and Tlili, 2008) can be further discriminated in some cases.

The XRDP spectra of the Solfatara new pool muds clearly indicate kaolinite and this is an important difference with the other muds containing smectites, and with most of the other samples as well (Fig. S1e vs. Fig. S1c,d). The DRIFT-FT-IR investigations on these kaolinite-bearing samples shows the characteristic shape (Madejova, 2003; Fitos et al., 2015) with two minor bands at 3667 and 3651 cm^{-1} between two major vibrational modes at 3695 and 3620 cm^{-1} (Fig. S2e; Table S2). The presence of all these bands suggests the absence (or paucity) of structural defect of kaolinite (Madejova et al., 2002). The rest of the infrared pattern is not simple because the overlapping signals from alunite and amorphous. Following Madejova et al. (2002), it is possible to reveal three strong bands (i.e., 1092-1097, 1026-1029, 1008-1012; Table S2) between 1100 and 1000 cm^{-1} (Fig. S2e) that lacks in the smectites-bearing muds and can derive from the kaolinite contribution. In agreement with the authors, the smectite in muds should produce the broad bands at around

1096-1095 cm^{-1}. Our results confirm the sensitivity of the FT-IR to detect kaolinite into clay mixtures (Madejova et al., 2002).

Otherwise, the DRIFT-FT-IR spectra are not resolute to determine the illite or montmorillonite contribution, particularly when present in low amount into mixtures of clays (Madejova et al., 2002), as in our case. We observe that the Pisciarelli smectite-bearing samples have a few band/hamp at around 3620 cm^{-1} (Fig. S2d) and this band is stronger in illite with respect to montomorillonite (Clark et al., 2007). However, the illite should produce signals between 4260 and 4090 cm^{-1}. These signals lack also in the infrared spectra of our Pisciarelli mud samples, probably due their small amount of smectites. Nevertheless, in absence of details on clays, we cannot exclude that the flat infrared traces in this region can be indicative of the montmorillonite or the illite/montmorillonite interlayer that characterize several samples (Fig. S1g). The Solfatara muds (Fig. S2c) produced infrared spectra very similar to those of smectites-bearing samples, and in particular display the band at 3620 cm^{-1}. Although the XRDP spectra of these muds do not present smectites-related peaks (Fig. S1c), the infrared spectra suggest further evaluations.

Evaporates from water collected at the Pisciarelli pools are mixtures of ammonium sulfates and mascagnite is dominant (Fig. S1a, Table S1). The mascagnite has the formula $(NH_4)_2SO_4$ and differently from other phases detected in the studied products (Table S1, 1) for the NH_4 group. According the literature (Basciano and Peterson, 2007), a sharp, clear band in the 1430-1450 cm^{-1} range of the infrared spectrum is the most accurate for identifying the NH_4-rich samples. This is also verified in ammonio-alunite and ammonio-jarosite series, the general formula of which, $(K,Na,NH_4)(Al,Fe)_3(SO_4)_2(OH)_6$, differs from our ammonium sulfates (Parafiniuk and Kruszewky, 2010) and in $(NH_4)_2SO_4$ particles (Weis and Ewing, 1996) that approach our mineral chemistry. A band at 1416 cm^{-1} characterizes the Mascagnite (sample GDS65.a) from the USGS database (Clark et al., 2007). Our mascagnite shows a well-defined infrared spectrum characterized by a sharp band at 1422-1411 cm^{-1} that is in the region of the $\nu_4(NH_4^+)$. Therein, we observe for other possible band correspondences between our infrared spectra and those reported in the cited literature. The results tabled below

	our sample $(NH_4)_2SO_4$ (cm^{-1})	Weis and Ewing, 1996 $(NH_4)_2SO_4$ (cm^{-1})	Parafiniuk and Kruszewky, 2010 $(K,Na,NH_4)(Al,Fe)_3(SO_4)_2(OH)_6$ (cm^{-1})	USGS $(NH_4)_2SO_4$ (cm^{-1})
$\nu_3(NH_4)$	3213-3200 3022 2870-2877	3216-3219 3050-3062 2850	3340-3100 ca. 3100 2850-2900	ca 3198 ca 3000
$\nu_4(NH_4^+)$	1422-1411	1421-1472	1430-1450	1416
$\nu_3(SO_4^{-2})$	1096	1113-1114	unclear	1106
$\nu_4(SO_4^{-2})$	614	620-621	unclear	618

evidence the bands at 1096 cm^{-1} and at 614 cm^{-1} that can be associated with $\nu_3(SO_4^{-2})$ and $\nu_4(SO_4^{-2})$, respectively. We also detect the three bands at 3213-3200 cm^{-1}, 3022 cm^{-1} and 2870-2877 cm^{-1} that can be linked to $\nu_3(NH_4)$ vibrational modes. Our mascagnite also includes a hump between 2491 and 2045 cm^{-1} that does not fit the $(NH_4)_2SO_4$ and instead can be detected in the Al-richer ammonio-alunite series where it is attributed to the ν(Al-OH) vibrational modes. We infer that the band should derive by small amount of tschermigite with formula $(NH_4)Al(SO_4)_2 \cdot 12(H_2O)$ that is common in our samples from Pisciarelli (Table S1).

The XRDP and FT-IR investigations on evaporates are very interesting when compared with their cognate muds. Based on XRDP spectra, NH_4-bearing species that characterize waters, seem absent in most of these muds. The muds decanted from the Pisciarelli pools are dominantly mixtures of alunite, pyrite, amorphous, variable amount of primary feldspars and illite/montmorillonite; only few muds present ammonium sulfates at the XRDP. Indeed, at the infrared spectroscopy, they produced the clear, sharp band at around 1430 cm^{-1} (Fig. S2d), i.e. in the region of the $\nu_4(NH_4^+)$ (Weis and Ewing, 1996; Parafiniuk and Kruszewski, 2010). This is an obvious result and demonstrates that, in some circumstances, FT-IR can be used to detected crystals that due the small abundance cannot be discriminable at the XRDP. The band also occurs in the Solfatara muds and we are confident on the attribution to the $\nu_4(NH_4^+)$ because the absence of other minerals detected in the assemblage that can produce signals at this wavelength.

Native S from two different samples (PINT S tozzo 18/10/17 and PINT S 18/1/18 in Table 1; Fig. S2b) produced DRIFT-FTIR spectra at the wavenumbers < 2950 cm^{-1}, with the strongest bands at 843 and 468 cm^{-1} that coincide with those of sulfur in the both the USGS (see Sulfur GDS94; Clark et al., 2007) and ruuff (http://rruff.info/) databases. The spectra differ in the OH stretching region, likely indicating the occurrence of impurities, although water absorption by the KBr solution can be a further possibility.

The FTIR results (not shown) on two samples for which whole-rock geochemistry testifies the richness in carbon (7 to 20 wt% on the total) show bands at 2850, 2920, 1455 and 1375 cm^{-1} attributable to C=H ligands (Glamoclija et al., 2004). These results indicate that the FT-IR allows a rapid check for eventual organic groups in samples and corroborate the absence of low to absence of such ligands in samples in Fig. S2.

Cited references

Basciano, L.C., and Peterson, R.C.; The crystal structure of ammoniojarosite, $(NH_4)Fe_3(SO_4)_2(OH)_6$ and the crystal chemistry of the ammoniojarosite–hydronium jarosite solid-solution series. Mineral Mag, 71, 427-441, 2007.

Clark, R.N., King, T.V.V., Klejwa , M., Swayze. G.A., and Vergo, N.: High spectral resolution reflectance spectroscopy of minerals, J. Geophys. Res., Solid Earth, 95, 12653-12680, doi:10.1029/JB095iB08p12653, 1990.

Clark, R.N., Swayze, G.A., Wise, R., Livo, E., Hoefen, T., Kokaly, R., and Sutley, S.J.: USGS digital spectral library splib06a: U.S. Geological Survey, Digital Data Series 231, http://speclab.cr.usgs.gov/spectral.lib06, 2007.

Fitos, M., Badogiannis, E.G., Tsivilis, S.G., and Perraki, M.: Pozzolanic activity of thermally and mechanically treated kaolins of hydrothermal origin, App. Clay Sci., 116–117, 182–192, doi:10.1016/j.clay.2015.08.028, 2015.

Glamoclija, M., Garrel, L., Berthon, J., and Lopez-Garcıa, P.: Biosignatures and bacterial diversity in hydrothermal deposits of Solfatara Crater, Italy, Geomicrobiol . J., 21, 529–541, doi:10.1080/01490450490888235, 2004.

Madejová, J.: FTIR techniques in clay mineral studies, Vib. Spectrosc., 31, 1–10, doi:10.1016/S0924-2031(02)00065-6, 2003.

Madejová, J., and Komadel, P.: Baseline studies of the clay minerals society source clays: infrared methods, Clays Clay Min, 49, 5, 410-432, 2001.

Madejová, J., Kečkéš, J., Pálková, H., and Komadel, P.: Identification of components in smectite/kaolinite mixtures. Clay Min, 37(2), 377-388, 2002.

Parafiniuk, J., and Kruszewky, L.: Minerals of the ammonioalunit-ammoniojarosite series e formed on a burning coal dump at Czerwionka, Upper Silesian Coal Basin, Mineral. Mag., 74(4), 731–745, doi:10.1180/minmag.2010.074.4.731, 2010.

Toumi, M., and Tlili, A.: Rietveld Refinement and Vibrational Spectroscopic Study of Alunite from El Gnater, Central Tunisia, Russian Journal of Inorganic Chemistry, 53, 1845–1853, 2008.

Weis, D. D., and Ewing, G. E.: Infrared spectroscopic signatures of $(NH_4)_2SO_4$ aerosols, J. Geoph. Res., 101, 18709-18720.

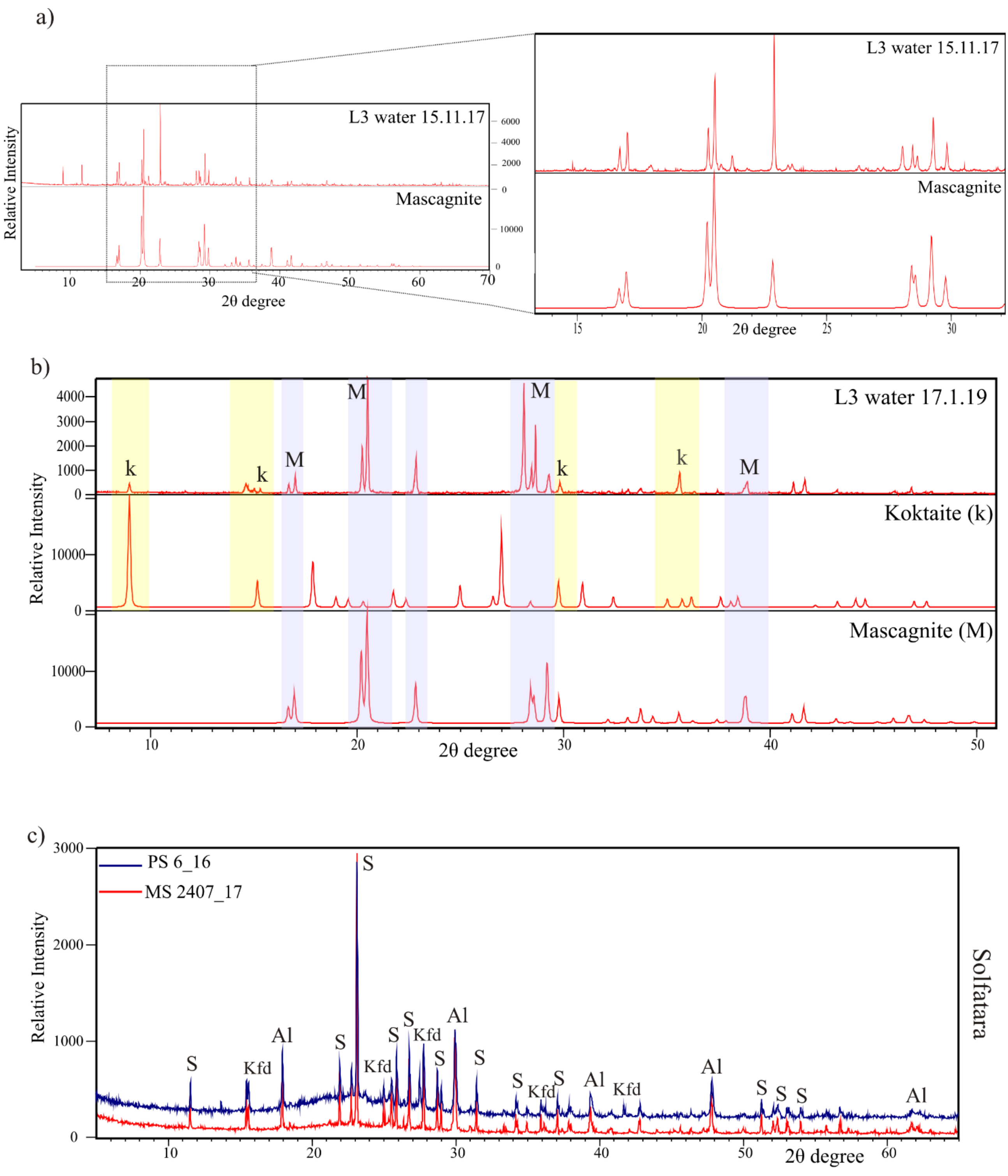
a)
L3 water 15.11.17
Mascagnite
Relative Intensity
2θ degree
b)
L3 water 17.1.19
Koktaite (k)
Mascagnite (M)
k
M
Relative Intensity
2θ degree
c)
PS 6_16
MS 2407_17
S
Kfd
Al
Relative Intensity
2θ degree
Solfatara

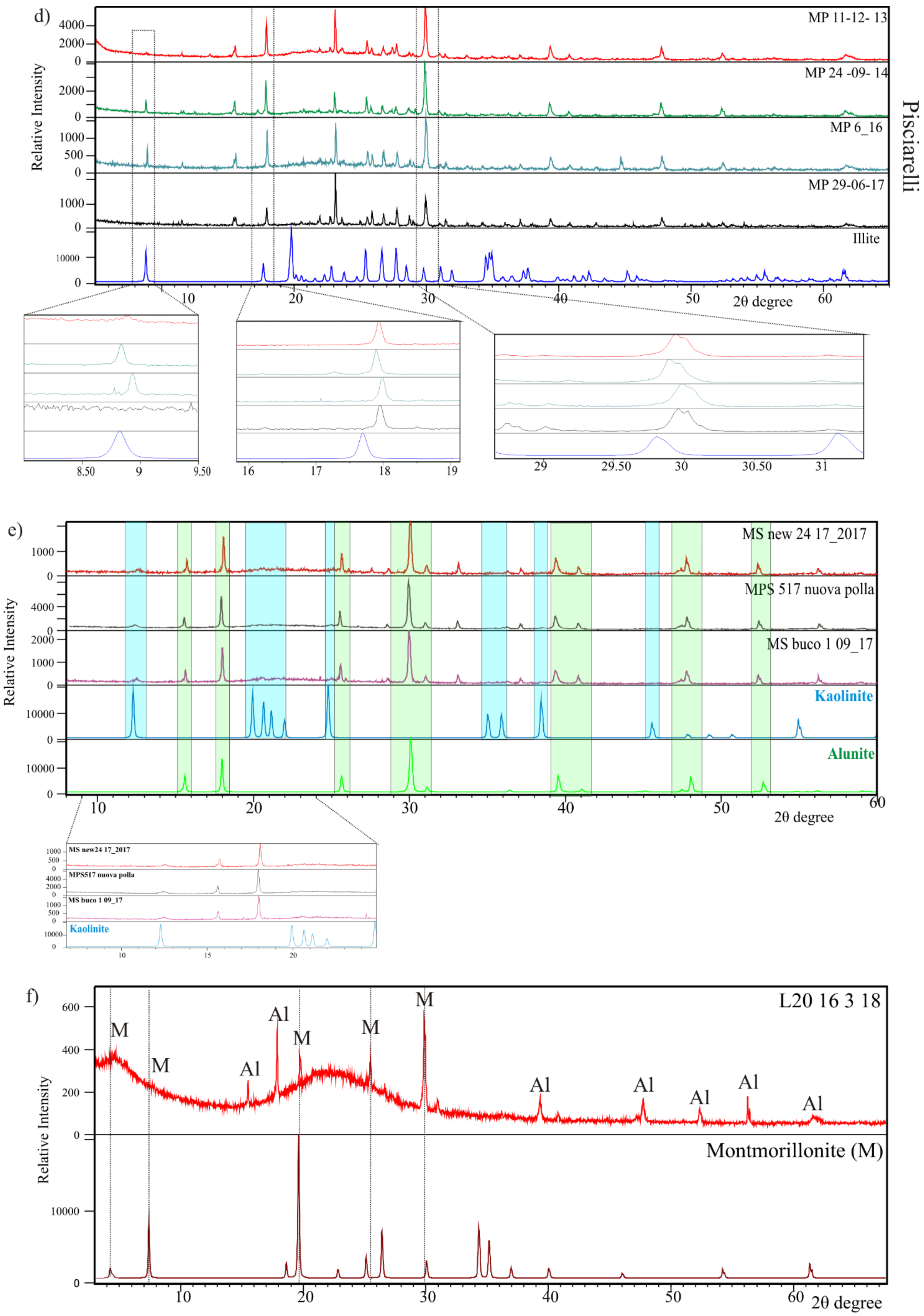
d)
Relative Intensity
MP 11-12- 13
MP 24 -09- 14
MP 6_16
MP 29-06-17
Illite
Pisciarelli
2θ degree
e)
Relative Intensity
MS new 24 17_2017
MPS 517 nuova polla
MS buco 1 09_17
Kaolinite
Alunite
2θ degree
f)
L20 16 3 18
M
Al
Montmorillonite (M)
Relative Intensity
2θ degree

Figure S1 – Representative XRDP spectra of NH_4- sulfates dominating the assemblage formed from drying the Pisciarelli water (a, b) and of various muds from Solfatara (c,e) and Pisciarelli (d,f). Each panel reports the sample name in Table S1. The muds show the large hump between 18 ° and 30 ° 2θ degree attributed to the amorphous phase. The smaller panels evidence the reflection intensity in the most significant range useful to discriminate illite in d) and kaolinites in e). Some XRDP spectrum has a corresponding infrared spectrum in Fig. S2: the sample with mascagnite is the same of Fig. S2a, the Solfatara muds in c) produced the FT-IR spectra in Fig. S2b, the Pisciarelli mud MP 6_16 is in Fig. S2d, the samples in e) are the same of Fig. S2e. Abbreviations (c, f): S = Sulfur; Al = Alunite; Kfd =Alkali feldspar.

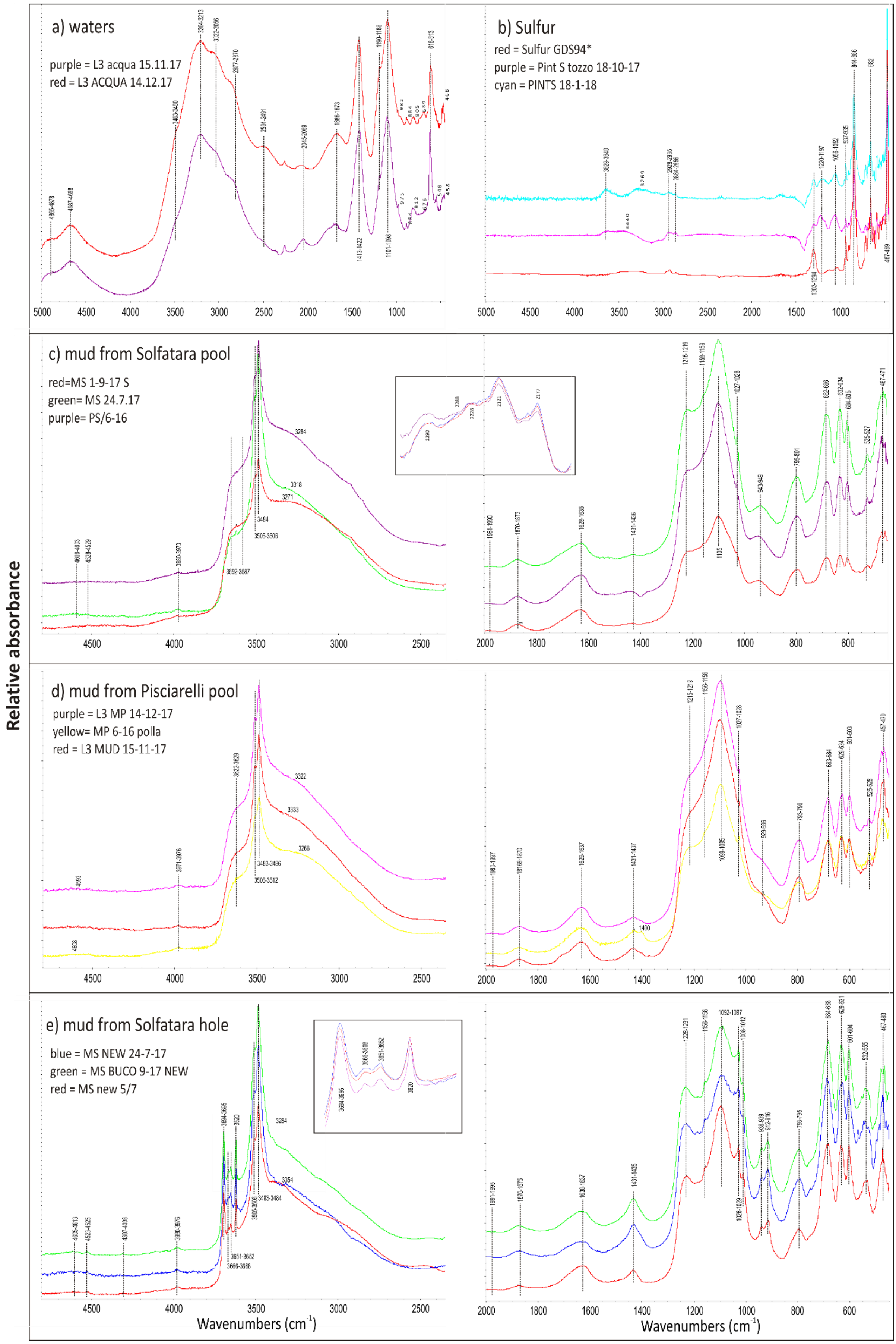

Figure S2 – FT-IR spectra of NH_4 - sulfates (a), native sulfur (b) and various muds from Solfatara (c), Pisciarelli (d) and the new Solfatara hole (e). See Table S2 for vibrational modes and relative assignments.